Effect of a metallic core on transient geomagnetic induction

J. Velímský,[1], C. C. Finlay[2]

[1] Department of Geophysics, Faculty of Mathematics and Physics, Charles University in Prague, V Holešovičkách 2, 180 00 Prague 8, Czech Republic

[2] Institut für Geophysik, ETH Zürich, Sonnegstrasse 5, 8092 Zürich, Switzerland

Abstract. Magnetic fields due to the magnetospheric ring current, together with their induced counterparts, must be correctly taken into account when modelling the geomagnetic field using modern observatory and satellite measurements. It is common practice to parameterize the induced field using a response function depending on a spherically symmetric electrical conductivity model of the solid Earth. Here, we show that Earth's metallic core should be included in such conductivity models which has not previously been the case. Abrupt changes in the amplitude of the ring current during geomagnetic storms excite a wide range of frequencies, some of which can induce electrical currents in the core. These currents decay very slowly due to the high conductivity of the core; the resulting induced field will therefore not be of zero mean even when averaged over many years. We present the results of time-domain numerical simulations of induction that demonstrate the influence of a conducting core in an idealized experiment based on a synthetic geomagnetic storm. Moving to a more realistic scenario we show that taking 50 years of $D_{\rm st}(t)$ index as an input, an induced field $I_{\rm st}(t)$ with a mean value (when averaged over 10 years) of up to $-1.5\,{\rm nT}$ is obtained. We conclude that transient induction in the metallic core caused by magnetospheric field variations must be included in accurate portrayals of the near-Earth magnetic environment.

1. Introduction

The observed geomagnetic field is a superposition of signals from a diverse range of sources. The largest component is due to the magnetohydrodynamic dynamo operating in Earth's liquid metal core which gives rise to geomagnetic secular variation on time scales of years to millennia [*Bloxham et al.*, 1989]. Remanent and induced magnetization in the Earth's lithosphere provides a contribution indicative of the local features of crustal geology [*Langel & Hinze*, 1998]. More rapid variations have their origin in the electrical currents flowing in the magnetosphere, such the ring current, tail currents, magnetopause currents [*Baumjohann & Treumann*, 1997], and in the ionosphere, for example, tidally driven solar quiet time currents, equatorial electrojets, auroral electrojets and polar cap currents etc. [*Kelley*, 2009]. Temporal variations of external fields in addition induce electrical currents within the electrically conducting solid Earth and oceans; these currents in turn give rise to secondary internal magnetic fields [see, for example, *Kuvshinov*, 2008]. Monitoring the geomagnetic field from satellites and the global network of magnetic observatories thus provides a wealth of information concerning both the solid Earth and the near-Earth solar-terrestrial environment. In addition, operational models of the slowly varying internal field, for example IGRF-11 [*Finlay et al.*, 2010], are widely used by individuals and by commercial organizations as a source of directional information. The accuracy of these models depends crucially on the ability to reliably separate contributions from these different sources.

A major challenge in geomagnetism today is to formulate appropriate models of the fields that originate in different sources. These representations should accurately and compactly capture their essential physics, and facilitate efficient separation of the various fields. In this study we

concentrate on one aspect of this enterprise, namely how induction in the solid Earth driven by variations in the magnetospheric ring current, could be better parameterized in geomagnetic field models.

Models of the present geomagnetic field now routinely include a basic parameterization of induction effects. These involve only the first order effects of induction driven by external field variations (assumed to be due to a symmetric ring current) acting on an electrically conducting upper mantle that is further assumed to be spherically symmetric. *Maus & Weidelt* [2004] and *Olsen et al.* [2005] independently proposed that an appropriate method of parameterizing this process was through use of the complex transfer function $\tilde{Q}_1(\omega)$ [see, for example, *Schmucker*, 1987] derived from a specified radial electrical conductivity profile. Within this framework the $D_{\rm st}(t)$ index (determined from measurements of the horizontal magnetic field intensity at the Hermanus, Kakioka, Honolulu, and San Juan magnetic observatories with an estimated baseline removed [*Sugiura & Kamei*, 1991]) is separated into an external part $E_{\rm st}(t)$ and an internal induced part $I_{\rm st}(t)$. This procedure is used in the majority of recent geomagnetic field models. For example it is the basis of the parameterization of induction effects in the CHAOS series of models [*Olsen et al.*, 2006, 2009, 2010] and also in the POMME series of models [*Maus et al.*, 2006, 2010; *Lühr & Maus*, 2010]. A very similar procedure but using the VMD index [*Thomson & Lesur*, 2007] rather than the $D_{\rm st}(t)$ index is used in the GRIMM series of field models [*Lesur et al.*, 2008, 2010].

All the geomagnetic field models mentioned above implicitly involve 1-D electrical conductivity models of the solid Earth such as that of *Utada et al.* [2003] that assume the Earth below 1000 km depth is a uniform, weakly conducting sphere. Though this assumption is very reasonable if one considers only rapid external field variations with time scales limited to periods less

than 100 days, we will demonstrate below that if the excitation field contains power at longer time scales, for example if a wide range of frequencies are excited during a magnetic storm, then one must use conductivity models including a conducting core in order to accurately model the induced magnetic field. When a conducting core is taken into account we will show that it is no longer necessary for the internal part of $D_{\rm st}(t)$, i.e. $I_{\rm st}(t)$, to have a zero mean, even when averaged over time scales longer than ten years. Thus geomagnetic storms are expected to give rise to small but noticeable induced internal fields even during magnetically quiet times, due to the long time taken for the induced currents in the core to decay.

2. Separation of time-domain $\mathbf{D_{st}}(t)$ index into external and internal parts

Maus & Weidelt [2004], and *Olsen et al.* [2005] showed how to separate $D_{\rm st}(t)$ into its internal part $I_{\rm st}(t)$ and its external part $E_{\rm st}(t)$ under the simplifying assumption that one is dealing with a purely dipolar source field and a spherically symmetric, electrically conducting, mantle. Working in the frequency domain if one is given the response function $\tilde{Q}_1(\omega)$, which depends only on the assumed electrical conductivity profile $\sigma(r)$, and $\tilde{D}_{\rm st}(\omega)$ (the Fourier transform of the $D_{\rm st}(t)$ index) then $\tilde{I}_{\rm st}$ (the Fourier transform of $I_{\rm st}(t)$) can be calculated by the relation

$$\tilde{I}_{\rm st}(\omega) = \frac{\tilde{Q}_1(\omega)}{1+\tilde{Q}_1(\omega)}\,\tilde{D}_{\rm st}(\omega). \tag{1}$$

In the time-domain, (1) is equivalent to a convolution,

$$I_{\rm st}(t) = \mathcal{F}^{-1}\left\{\frac{\tilde{Q}_1(\omega)}{1+\tilde{Q}_1(\omega)}\right\}(t) * D_{\rm st}(t), \tag{2}$$

where $\mathcal{F}^{-1}$ denotes the inverse Fourier transform.

In this study we work in the time-domain using the methodology developed by *Velímský & Martinec* [2005]. This enables us to efficiently study the transient response of the system and to work directly with the $D_{\rm st}(t)$ time series. *Martinec & McCreadie* [2004] have shown that in the

time-domain the EM induction forward problem can be formulated with a Dirichlet boundary condition, where the horizontal component of magnetic field is prescribed at the satellite altitude. We modified the code of *Velímský & Martinec* [2005] to impose this boundary condition directly at the Earth's surface. In particular, we match the prescribed time-dependent dipolar coefficient of the horizontal magnetic field using the $D_{\rm st}(t)$ index,

$$X_{10}(t) = D_{\rm st}(t) = E_{\rm st}(t) + I_{\rm st}(t). \tag{3}$$

Note that according to the definition of $D_{\rm st}$, the problem is formulated in the geomagnetic (dipolar) coordinate system, i.e.,

$$X(\vartheta;t) \;=\; X_{10}(t)\frac{\partial P_{10}(\cos\vartheta)}{\partial\vartheta}, \tag{4}$$

$$Y(\vartheta;t) \;=\; 0, \tag{5}$$

where ϑ is geomagnetic colatitude, X, and Y are components of the magnetic field oriented towards geomagnetic north and east, respectively, and $P_{10}(\cos\vartheta)$ is degree 1 Legendre polynomial.

Given this boundary condition, and a conductivity profile, the forward modelling scheme predicts the time-dependent dipolar coefficient of the vertical field, $Z_{10}(t)$, for which

$$Z_{10}(t) = E_{\rm st}(t) - 2\,I_{\rm st}(t). \tag{6}$$

This coefficient is related to the downward component of magnetic field by

$$Z(\vartheta;t) = Z_{10}(t)P_{10}(\cos\vartheta). \tag{7}$$

By combining Eqs. (3) and (6), we obtain

$$I_{\rm st}(t) = \frac{D_{\rm st}(t) - Z_{10}(t)}{3}, \tag{8}$$

and, obviously,

$$E_{\rm st}(t) = D_{\rm st}(t) - I_{\rm st}(t). \tag{9}$$

Note that since we are dealing with a finite, discretely sampled, transient signal, the equivalence of frequency-domain approach (1), and the time-domain approaches (2) or (3–8) is subject to both the Shannon sampling theorem and the Paley-Wiener theorem [*Papoulis*, 1984, p.188]. In particular, if we cannot resolve the spectrum $\tilde{D}_{\rm st}(\omega)$ at very low frequencies, i.e., for periods much longer than the length of the signal $D_{\rm st}(t)$ in the time domain, then equation (1) will not accurately predict the induced field $\tilde{I}_{\rm st}(\omega)$ in this period range. The results of $D_{\rm st}(t)$ separation in the time-domain using any realistic signal can be affected by a switch-on effect that occurs at the start of the integration. The EM induction solver has to be provided with an initial condition — a snapshot of magnetic field everywhere in the Earth. For no better source of information, this is assumed to be zero [*Velímský & Martinec*, 2005].

3. Results

3.1. Conductivity models and their respective induction responses

In this study we explore the influence of a range of possible 1-D conductivity models obtained by inversion of data from magnetic observatories, submarine cables, and low-orbit satellites (Figure 1 and Table 1). Model U is a semi-global model derived by *Utada et al.* [2003] from observatory and cable data for Pacific hemisphere. It was previously used to separate the external and internal fields both by *Maus & Weidelt* [2004] and *Olsen et al.* [2005]. *Kuvshinov & Olsen* [2006] inverted five years of CHAMP, Ørsted, and SAC-C satellite measurements to obtain the global conductivity model K. We also consider the conductivity model O derived by *Olsen* [1999] from European observatory data. In all these models, the homogeneous conductivity of

the lower mantle, below a depth of 1500 km, is extended down to the centre of Earth. In addition we also consider three models called UC, OC, and KC, that include an electrically conducting core with radius 3480 km, and uniform conductivity $10^5\,\mathrm{S\,m^{-1}}$.

The high-temperature and high-pressure measurements of electrical conductivity of iron alloys provide us with estimates of the core conductivity within the range of 10^5–$10^6\,\mathrm{S\,m^{-1}}$, where the content of impurities in the core material is likely the major source of uncertainty [*Stacey*, 2007; *Stacey & Loper*, 2007]. Therefore, we finally study an additional model, UC6, also based on Utada's mantle conductivity profile, but with the core conductivity increased to the value of $10^6\,\mathrm{S\,m^{-1}}$. We expect that while the UC, OC, and KC models will provide us with conservative estimates of the core effect on the internal field separation, model UC6 will yield an upper limit.

Although we work in the time-domain, which we believe is preferable for computing transient responses, it nonetheless provides useful insight to first discuss the conventional frequency-domain $\tilde{Q}_1$-responses. In the right panel of Figure 1 we present the amplitude responses, computed from each conductivity model using a 1-D spherical solver [*Pěč et al.*, 1985]. In the period range between 1 day and 1 year, the differences between the various conductivity models are negligible for the purpose of internal - external field separation. At shorter periods, the continental and oceanic models deviate slightly from the global satellite model K in opposite directions. However, the most striking feature of Figure 1 is the difference between models with and without the highly conductive core at periods longer than 1 year. The core significantly slows down the decrease of $\tilde{Q}_1(\omega)$ amplitudes. In the presence of a conducting core, as can be understood from simple arguments related to the magnetic diffusion timescale of the core [*Everett & Martinec*, 2003; *Gubbins & Roberts*, 1987], it is only at periods greater than 10^5 years

(and even more in the case of UC6 model) that the amplitude of the induced response drops to zero.

3.2. Induction in the core due to an idealized geomagnetic storm

Next, we demonstrate the influence of a highly conductive core in the time-domain using a simple synthetic model of an isolated geomagnetic storm. Following *Everett & Martinec* [2003], we use an exponential decay model,

$$D_{\mathrm{st}}(t) = H(t)\, \exp(-\alpha t), \tag{10}$$

where $H(t)$ is the Heaviside step function, and $1/\alpha = 4\,\mathrm{days}$ is the decay time of a typical storm [*McPherron*, 1995]. Thanks to the linearity of the EM induction problem with respect to the Dirichlet boundary condition, the results of induced field separation can be easily rescaled from the synthetic example with unitary peak value to realistic amplitudes.

Figure 2 shows how the induced field index $I_{\mathrm{st}}(t)$ can be separated in the time-domain, using the approach described by equations (3–8), for conductivity models U, UC, and UC6, respectively. The effect of including the core is clearly visible. Note that $I_{\mathrm{st}}(t)$ for all three conductivity models crosses the zero from positive to negative values at $t_0 = 11\,\mathrm{days}$, but later zero crossings appear at different times, depending on the conductivity model. Similar results were obtained for models O, OC, K, and KC, they are omitted for the sake of simplicity.

Further insight is obtained by calculating the dependence of average value of $I_{\mathrm{st}}(t)$,

$$\langle I_{\mathrm{st}} \rangle_{(0,\tau)} = \frac{1}{\tau} \int_0^{\tau} I_{\mathrm{st}}(t)\, \mathrm{d}t, \tag{11}$$

on the averaging length τ, as shown in the bottom plot of Figure 2. Averaging over 50 years yields a signal of at least 10^{-5} in the presence of the core (both in models UC and UC6). This is three orders of magnitude more than in the case without core. For a typical storm with negative

peak value of the order of $-10^2\,\mathrm{nT}$, and occurring about 10^3 times within the 50 year interval, we can thus expect a negative shift of the time-averaged signal on the order of a few of nT, if a conductive core is present.

3.3. Time-domain separation of $D_{\mathrm{st}}(t)$ into external and induced parts

Next, we move to a more realistic scenario taking the D_{st} index as input for our simulations. We work with a 50 year-long time series of the definitive D_{st} index (`ftp://ftp.ngdc.noaa.gov/STP/GEOMAGNETIC_DATA/INDICES/EST_IST/`), starting on January 1, 1957, 0:00 UTC. The first value of D_{st} in this time series is +12 nT. Starting from a zero initial condition would thus introduce an artificial jump of 12 nT at the first step of the time integration. To avoid this artificial transient effect, we instead begin the time integration at 17:00 UTC on the same day, when D_{st} reaches zero for the first time. We have tested starting the simulation from other zero D_{st} values occuring during 1957. This has no effect on presented results for conductivity models both with and without the core.

Another important factor affecting our results is the baseline value of D_{st}. Simulating the response of the system to a Heaviside step loading at $t = 0$ shows that for every 1 nT of constant shift of D_{st}, there is an average shift of $I_{\mathrm{st}}(t)$ by 0.1 nT in the presence of the core due to much larger effectivity of the Heaviside loading at very long periods, compared to the exponential storm model. This demonstrates the importance of the D_{st} baseline value.

We use D_{st}(t) to excite all seven conductivity models introduced in Section 3.1. Figure 3 shows the resulting I_{st} averages, using window lengths of 1 month, 1 year, and 10 years, respectively. There is a persistent systematic shift by -1 to $-1.5\,\mathrm{nT}$ present in all models including the core, although for the shortest averaging length it is dwarfed by the short-time variations of external field. When 1 year averaging length is used, the 11 year solar cycle period is also pronounced.

The long-term decrease of $\langle I_{\rm st} \rangle_{10\,\rm y}$ between years 1967–1990 is also present in $\langle D_{\rm st} \rangle_{10\,\rm y}$. It is observed only in models UC, UC6, KC, and OC. Without the conductive core, the models U, O, and K are insensitive to the long-period characteristics of $D_{\rm st}$. Though inclusion of a highly conductive core increases the differences between different mantle conductivity models, this effect is rather minor. The effect of uncertainty in core conductivity is also rather unimportant, provided it remains within the range of 10^5–$10^6\,\mathrm{S\,m^{-1}}$. We also recall that the inclusion of the core shifts the running averages of $E_{\rm st}$ by exactly the same amount, as the corresponding averages of $I_{\rm st}$, but in the opposite direction. This is a direct implication of equation (3).

A possible difficulty with this experiment is that $D_{\rm st}(t)$ is known to have shortcomings on long timescales of months to years. This sometimes motivates the detrending $D_{\rm st}(t)$ prior to it's use for field modelling [*Olsen et al.*, 2005]. However, such pre-processing is not suitable for the time-domain approach because it gives rise to a substantial switch-on effect discussed above. Irrespective of whether or not $D_{\rm st}(t)$ is an imperfect driving source, the physical effect of large geomagnetic storms inducing slowly decaying currents in the core seems unavoidable.

4. Concluding remarks

Time variations of the magnetospheric ring current, in particular due to intense geomagnetic storms, are capable of inducing secondary electric currents in the Earth's core. We have demonstrated that this effect is observable in the geomagnetic field at the Earth's surface. Since no electromagnetic induction occurs at zero frequency, the mean value of the $I_{\rm st}(t)$ index characterizing the induced field at the surface should tend to zero. However, in the Earth with its highly conductive core, this is true only for averages over very long time intervals, much longer than the observation times of relevance here. Averaging the $I_{\rm st}(t)$ index over shorter time windows yields a non-zero shift, of order of a few nT, to negative values. Throughout

this study it has been assumed that the core is a stationary conductor rather than a liquid metal. But in reality the outer core will likely respond to the perturbations produced by geomagnetic storm events through the excitation of magnetohydrodynamic waves [see, for example *Jault & Légaut*, 2005; *Légaut*, 2005]. These will likely dissipate energy on time scales more rapid than the magnetic diffusion time scale of a solid core, but it will nonetheless take many years for the associated currents to decay. Further work is required to clarify this process.

The choice of particular mantle conductivity model used in the separation of external and internal fields was found to be of only secondary importance. On the other hand, our results indicate that a highly conductive core should be taken into account when one performs the decomposition into $I_{\rm st}(t)$ and $E_{\rm st}(t)$ that forms an essential input to modern geomagnetic field models. The non-zero offset value of $I_{\rm st}(t)$ will result in small change in the lowest degree internal Gauss coefficients of geomagnetic field models. In addition, slow (month to decade time scale) variations of $I_{\rm st}(t)$ will affect estimates of the secular variation and secular acceleration of the core field. Time series of $I_{\rm st}(t)$ and $E_{\rm st}(t)$ produced using the methods described here with the U, UC, and UC6 models may be found online at `http://geo.mff.cuni.cz/~velimsky/Dst_separation/`. For transient time series of limited length, which contain long-period signal components, the time-domain approach via numerical integration of the EM induction equation may be better suited than a frequency-domain decomposition.

Acknowledgments. J.V. acknowledges the support of the Grant Agency of the Czech Republic, projects No. 205/08/P229, P210/11/1366. We thank Stefan Maus, Mark Everett, Alexei Kuvshinov, Dominique Jault, Ivo Oprš al, and František Gallovič for helpful discussions. Constructive comments by Vincent Lesur and one anonymous reviewer are also appreciated.

References

Bloxham, J., D. Gubbins, and A. Jackson, 1989, Geomagnetic secular variation, *Philos. Trans. Roy. Soc. Lond. A., 329,* 415–502.

Baumjohann, W., & R.A. Truemann, 1997, Basic Space Plasma Physics, Imperial College Press, ISBN 1-86094-079-X.

M. Everett, & Z. Martinec, 2003, Spatiotemporal response of a conducting sphere under simulated geomagnetic storm conditions *Phys. Earth Plan. Int., 138,* 163–181.

D. Gubbins, and Roberts, P.H. 1987, Magnetohydrodynamics of the Earth's Core, *in Geomagnetism Volume 2, Edited J. A. Jacobs* 1–183.

C. C. Finlay, S. Maus, C. D. Beggan, T. N. Bondar, A. Chambodut, T.A. Chernova, A. Chulliat, V. P., Golovkov, B. Hamilton, M. Hamoudi, R. Holme, G. Hulot, W. Kuang, B. Langlais, V. Lesur, F. J. Lowes, H. Lühr, S. Macmillan, M. Mandea, S. McLean, C. Manoj, M. Menvielle, I. Michaelis, N. Olsen, J. Rauberg, M. Rother, T.J. Sabaka, A. Tangborn, L. Tøffner-Clausen, E. Thébault, A.W.P. Thomson, I. Wardinski, Z. Wei, and T.I. Zvereva, 2010, International Geomagnetic Reference Field: the eleventh generation, *Geophys. J. Int., 183(3),* 1216–1230.

Jault D. and G. Légaut, 2005, Alfvén waves within the Earth's core, *In: Fluid Dynamics and Dynamos in Astrophysics and Geophysics,* Volume editors A.M. Soward, C.A. Jones, D.W. Hughes, N.O. Weiss (The Fluid Mechanics of Astrophysics and Geophysics), CRC Press, 277–293.

Kelley, M. C., 2009, The Earth's Ionosphere. Plasma Physics and Electrodynamics, Academic Press, ISBN 13: 978-0-12-088425-4.

Kuvshinov, A.V. & N. Olsen, 2006, A global model of mantle conductivity derived from 5 years of CHAMP, Ørsted, and SAC-C magnetic data, *Geophys. Res. Lett., 29,* 139–186, doi:

10.1007/s10712-008-9045-z.

Kuvshinov, A.V., 2008, 3-D Global Induction in the Oceans and Solid Earth: Recent Progress in Modeling Magnetic and Electric Fields from Sources of Magnetospheric, Ionospheric and Oceanic Origin, *Surveys in Geophysics, 33,* L18301, doi: 10.1029/2006GL027083.

Langel, R. A., & W.J. Hinze, 1998, The Magnetic Field of Earth's Lithosphere. The Satellite Perspective, Cambridge University Press, ISBN 0-521-47333-0.

Légaut, G., Ondes de torsion dans le noyau terrestre, Ph.D. thesis, Univeristé Joseph Fourier, Grenoble, 2005.

Lesur, V., I. Wardinski, M. Rother, and M. Mandea, 2008, GRIMM: the GFZ Reference Internal Magnetic Model based on vector satellite and observatory data *Geophys. J. Int., 173,* 382–394.

Lesur, V., I. Wardinski, M. Hamoudi, and M. Rother , 2010, The second generation of the GFZ Reference Internal Magnetic Model: GRIMM-2, *Earth, Planets, Space, 62(10),* 765–773.

Lühr, H. & S. Maus, 2010, Solar cycle dependence of quiet-time magnetospheric currents and a model of their near-Earth magnetic fields, *Earth, Planets, Space, 62(10),* 843–848.

Martinec, Z. & H. McCreadie, 2004, Electromagnetic induction modeling based on satellite magnetic vector data, *Geophys. J. Int., 157,* 1045–1060.

Maus, S. & P. Weidelt, 2004, Separating the magnetospheric disturbance magnetic field into external and transient internal contributions using a 1D conductivity model of the Earth, *Geophys. Res. Lett., 31,* L12614, 2004.

Maus, S., C. Manoj, J. Rauberg, I. Michaelis, and H. Lühr, 2010, NOAA/NGDC candidate models for the 11th generation International Geomagnetic Reference Field and the concurrent release of the 6th generation POMME magnetic model, *Earth, Planets, Space, 62(10),* 729–735.

Maus, S., and M. Rother, C. Stolle, W. Mai, S. Choi, H. Lühr, D. Cooke and C. Roth, 2010, Third generation of the Potsdam Magnetic Model of the Earth (POMME), *Geochem., Geophys., Geochem. Geosys, 7* Q07008, doi:10.1029/2006GC001269.

McPherron, R.L., 1995, Magnetospheric dynamics. *In: Kivelson, M.G., Russell, C.T. (Eds.), Introduction to Space Physics,* Cambridge University Press, Cambridge, pp. 400–458.

Olsen, N., 1999, Long-period (30 days–1 year) electromagnetic sounding and the electrical conductivity of the lower mantle beneath Europe, *Geophys. J. Int., 138,* 179–187.

Olsen, N., T.J. Sabaka, and F.J. Lowes, 2005, New parameterization of external and induced fields in geomagnetic field modeling, and a candidate model for IGRF 2005, *Earth Planets Space, 57,* 1141–1149.

Olsen, N., H. Lühr, T.J. Sabaka, M. Mandea, M. Rother, L. Tøffner-Clausen and S. Choi, 2006, CHAOS – A model of the Earth's magnetic field derived from CHAMP, Ørsted, and SAC-C magnetic satellite data, *Geophys. J. Int., 166,* 67–75.

Olsen, N., Mandea, M., T.J. Sabaka, and L. Tøffner-Clausen, 2009, CHAOS-2 – A geomagnetic field model derived from one decade of continuous satellite data, *Geophys. J. Int., 179,* 1477—1487.

Olsen, N., M. Mandea, T.J. Sabaka, and L. Tøffner-Clausen, 2010, The CHAOS-3 geomagnetic field model and candidates for the 11th generation IGRF, *Earth, Planets, Space, 62(10),* 719–727..

Papoulis, A, 1984, Signal Analysis, International Edition, McGraw-Hill, ISBN 0-07-048460-0.

Pěč, K., Z. Martinec, and J. Pěčová, 1985, Matrix approach to the solution of electromagnetic induction in a spherically layered earth, *Studia Geophysica et Geodaetica, 29(2),* 139–162.

U. Schmucker, 1987, Substitute conductors for electromagnetic response estimates, *PAGEOPH., 125,* 341–367.

Stacey, F.D., 2007, Core, electrical conductivity, *In: Gubbins, D. and E. Herrero-Bervera (Eds.), Encyclopedia of Geomagnetism and Paleomagnetism,* Springer, Dordrecht, pp. 116–117.

Stacey, F.D., and D.E. Loper, 2007, A revised estimate of the conductivity of iron alloy at high pressure and implications for the core energy balance, *Phys. Earth Plan. Int. 161,* 13–18.

Sugiura M., & Kamei, T., 1991, Equatorial Dst index 1957–1986, *IAGA Bull. 40, edited by A. Berthelier and M. Menvielle, ISGI Publ. Off., Saint-Maur-des-Fossés, France, 1991.* http://wdc.kugi.kyoto-u.ac.jp/dstdir/dst2/onDstindex.html.

Thomson, A.W.P. & V. Lesur, 2007, An improved geomagnetic data selection algorithm for global geomagnetic field modelling *Geophys. J. Int., 169,* 951–963.

Utada, H., T. Koyama, H. Shimizu, and A.D. Chave, 2003, A semi-global reference model for electrical conductivity in the mid-mantle beneath the north Pacific, *Geophys. Res. Lett., 30,* 43–46.

Velímský, J. & Z. Martinec, 2005, Time-domain, spherical harmonic-finite element approach to transient three-dimensional geomagnetic induction in a spherical heterogeneous Earth, *Geophys. J. Int., 160,* 81–101.

Table 1. Overview of conductivity models used in this study.

label	reference	region	primary data source	σ_{core} (S m^{-1})
U	*Utada et al.* [2003]	Pacific	observatories, submarine cables	1.00
UC	*Utada et al.* [2003]	Pacific	observatories, submarine cables	10^5
UC6	*Utada et al.* [2003]	Pacific	observatories, submarine cables	10^6
O	*Olsen* [1999]	Europe	observatories	1.46
OC	*Olsen* [1999]	Europe	observatories	10^5
K	*Kuvshinov & Olsen* [2006]	global	satellites	2.21
KC	*Kuvshinov & Olsen* [2006]	global	satellites	10^5

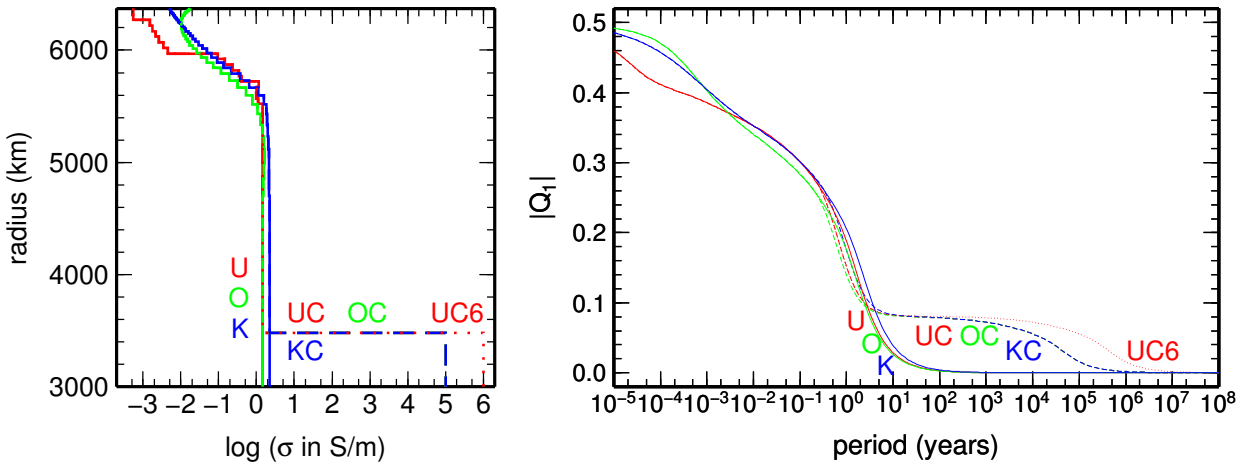

Figure 1. Left: Spherically symmetric conductivity models U, O, K, (red, green, and blue solid lines, respectively); models including a conductive core, UC, OC, and KC (red, green, and blue dashed lines, respectively); and model UC6 using upper estimate of core conductivity (red dotted line). Right: Corresponding amplitudes of $\tilde{Q}_1$ responses as functions of period/frequency.

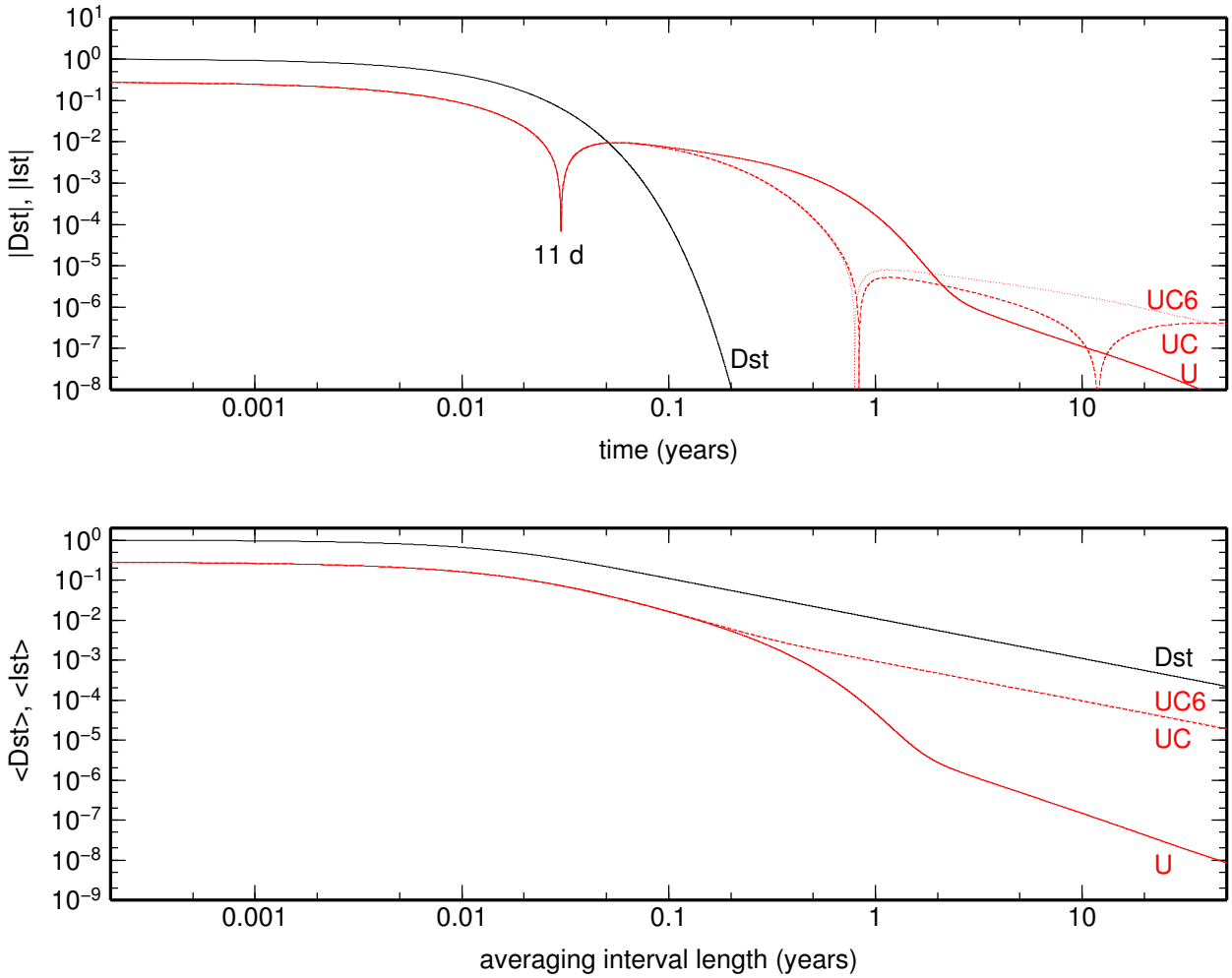

Figure 2. Induction by the exponential synthetic storm model. The top figure shows the $D_{\rm st}(t)$ index, and the $I_{\rm st}(t)$ indices obtained for conductivity models U, UC, and UC6, respectively. The bottom figure shows the dependence of average values of $D_{\rm st}(t)$, and $I_{\rm st}(t)$ on the length of averaging interval. Synthetic $D_{\rm st}(t)$ is shown in black, synthetic $I_{\rm st}(t)$ is in red, using solid, dashed, and dotted lines for respective conductivity models.

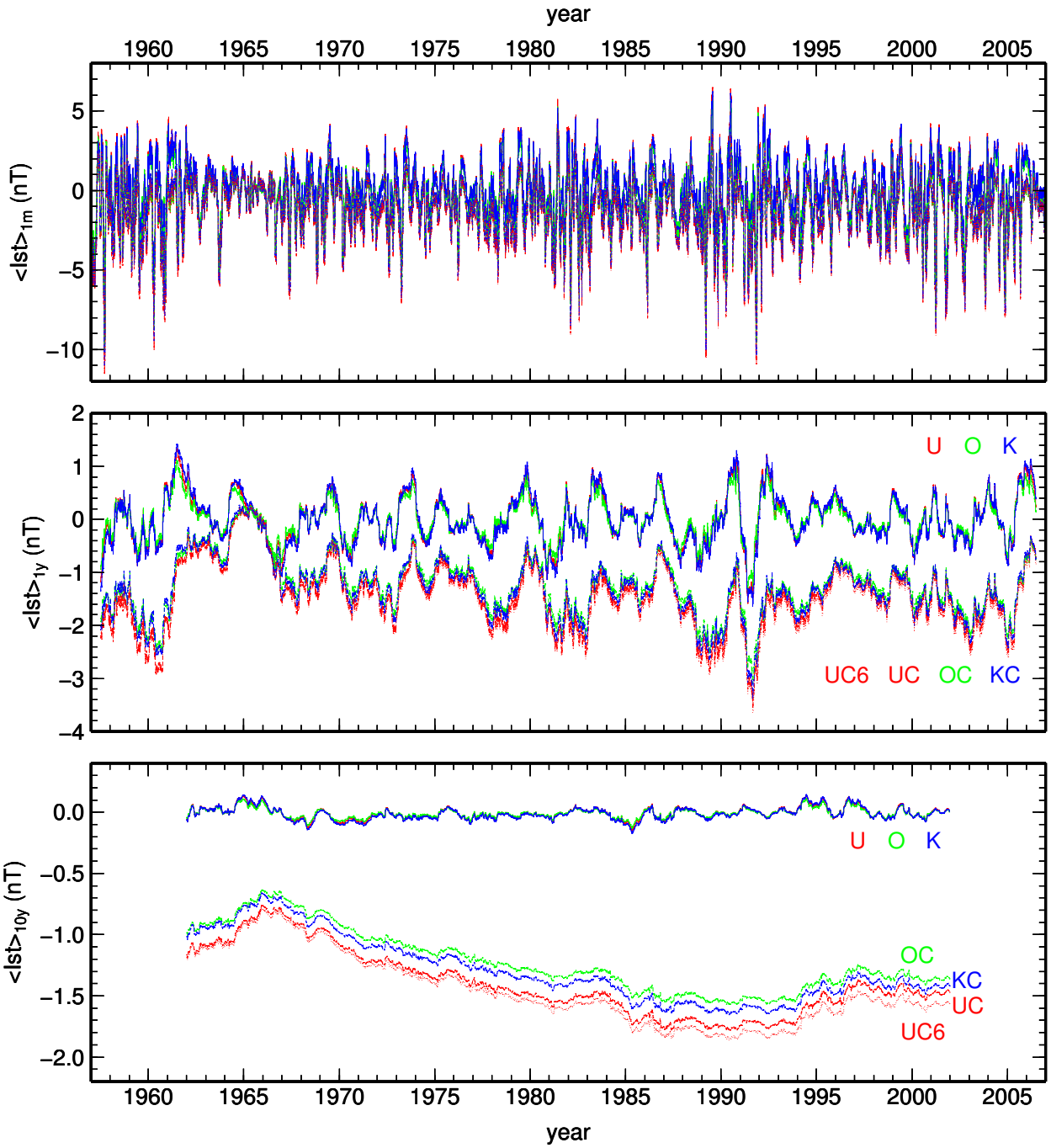

Figure 3. Moving averages of $I_{\rm st}(t)$ index obtained for various conductivity models excited by $D_{\rm st}(t)$. Window lengths of 1 month, 1 year, and 10 years are used respectively in the top, middle, and bottom figures. Color coding of lines corresponds to Figure 1.